AD-A049 983 JAYCOR DEL MAR CALIF F/G 20/4

NUMERICAL CALCULATION OF THE STABILITY OF PARALLEL FLOWS.(U)

DEC 77 J H STUHMILLER F49620-77-C-0030

UNCLASSIFIED AFOSR-TR-78-0062 NL

1 OF 1

AD
A049 983

END
DATE
FILMED
3-78
DDC

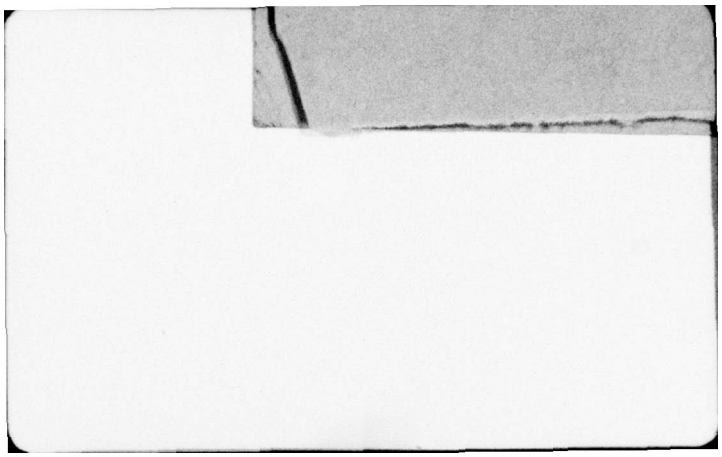

2

NUMERICAL CALCULATION OF THE STABILITY OF PARALLEL FLOWS

See back page for 1473

Final Report

Contract No. F49620-77-C-0030

December 5, 1977

Prepared By

James H. Stuhmiller

For

Space and Missile Systems Organization
and the
Air Force Office of Scientific Research

DDC
RECEIVED
FEB 15 1978
B

DISTRIBUTION STATEMENT A

Approved for public release;
Distribution Unlimited

JAYCOR; 1401 CAMINO DEL MAR (P.O. BOX 370); DEL MAR, CA 92014
(714) 453-5680

AIR FORCE OFFICE OF SCIENTIFIC RESEARCH (AFSC)
NOTICE OF TRANSMITTAL TO DDC
This technical report has been reviewed and is
approved for public release IAW AFR 190-12 (7b).
Distribution is unlimited.
A. D. BLOSE
Technical Information Officer

CONTENTS

	Page
ABSTRACT	ii
LIST OF SYMBOLS	iii
LIST OF FIGURES	iv
1. INTRODUCTION	1
2. THE MATHEMATICAL FORMULATION	3
3. THE NUMERICAL SOLUTION TECHNIQUE	7
4. COMPARISON WITH LINEAR STABILITY THEORY	15
5. FINITE AMPLITUDE EFFECTS	25
6. CONCLUDING REMARKS	29
7. ACKNOWLEDGEMENTS	30
8. REFERENCES	31

ACCESSION for
NTIS White Section ☑
DDC Buff Section ☐
UNANNOUNCED ☐
JUSTIFICATION
BY
DISTRIBUTION/AVAILABILITY CODES
Dist. AVAIL. and/or SPECIAL
A

ABSTRACT

A numerical approach to solving the two-dimensional, incompressible Navier-Stokes equations is presented and is used to study the stability and evolution of disturbances in a boundary layer. Previous numerical approaches have used streamfunction-vorticity formulations that take advantage of the special properties of two-dimensional flow. The present method solves a finite-difference form of the momentum equations and may therefore be extended to three-dimensions more readily. Computations using this technique are compared with the result of linear stability theory for small amplitude disturbances and are found to give satisfactory agreement, while calculations at large amplitude support the conjecture that non-linear effects can be destabilizing.

LIST OF SYMBOLS

Roman

i	index denoting cell columns
I	index of right-most columns
j	index denoting cell rows
J	index of top-most row
n	index denoting time level
p,P	fluid pressure divided by mass density
R	Reynolds number $(U_\infty \delta/\nu)$
T	period of oscillation of disturbance
u,U	streamwise component of fluid velocity
U_∞	free-stream velocity
x	streamwise coordinate
y	normal coordinate

Greek

α	dimensionless wavenumber $(2\pi\delta/\lambda)$
β	dimensionless frequency of oscillation $(2\pi\delta/U_\infty T)$
δ	momentum thickness of boundary layer
$\delta x, \delta y, \delta t$	finite space and time increments
∇^2	Laplacian operator $(\partial^2/\partial x^2 + \partial^2/\partial y^2)$
θ	logarithm energy change
λ	wavelength of disturbance
ν	kinematic viscosity of fluid
π	3.1415926 . . .

LIST OF FIGURES

Figure		Page
1.	A Typical Finite-Difference Mesh Configuration	8
2.	Variable Placement Within a Finite-Difference Cell	9
3.	Neutral Stability Curve and Cases for which Numerical Calculations have been made. Numbers indicate the logarithmic energy change per period	16
4.	Time variation of the flow energy for several numerical calculations	18
5.	Comparison of Production and Dissipation Rates During the Relaxation to a Final State for a Case Near the Neutral Curve	19
6.	Time Traces of the Horizontal Velocity Component for Various Distances from the Wall	22
7.	Comparison of Horizontal Velocity Amplitude Variation	23
8.	Comparison of Horizontal Velocity Phase Variation	24
9.	Variation of Energy with Time for Various Amplitudes of the Initial Disturbance	26
10.	Variation of Production and Dissipation Rates for Various Initial Disturbance Amplitudes	27

INTRODUCTION

One of the principal interactions between a fluid and a solid structure is the tangental force due to relative motion. At low velocities, when the flow is still laminar, the drag force is small, but at higher speeds, when the flow has become turbulent, the drag, as well as the heat transfer, increases enormously. It is of practical interest to be able to understand the mechanisms leading to the transition from a laminar to turbulent flow and to be able to predict and control that phenomena.

The onset of turbulence is preceeded by a motion in the boundary layer that is certainly three-dimensional and probably highly nonlinear. Any theory that would explain the transition process must address these two issues in some manner. At its initial stages, however, transition appears to involve fairly regular, small amplitude, two-dimensional disturbances that are capable of extracting energy from the mean flow and thereby grow rapidly. This motion is within the power of analysis to investigate as an eigenvalue problem and, consequently, it has been extensively studied.

The extension of these results to true initial value problems, large amplitudes, and three-dimensions has proven to be quite difficult for analysis and so it is desirable to develop other approaches to assist in understanding these effects. One promising approach is the direct, numerical solution of the governing equations. Encouraging results have already been obtained by Fasel (1976) and Murdock (1977) using a stream-function-vorticity formulation of the equations of motion. Fasel employed a three-time-level finite-difference solution

algorithm, while Murdock has combined an orthogonal function expansion in one spatial direction with a finite-difference formulation in the other. The two methods appear to give good agreement with linear analysis and with one another.

The present work explores another numerical approach: the finite-difference solution of the momentum form of the Navier-Stokes equations. Three variables (two velocities and a pressure) must now be calculated instead of two (a streamfunction and vorticity), however, the numerical technique is readily extended to three-dimensions where the concept of a streamfunction is no longer valid. The finite-difference algorithm used differs from that of Fasel in two respects. The present scheme introduces no numerical viscosity into the solution, while Fasel's scheme is slightly dissipative. Secondly, the present scheme requires storing the flow information at only one time level, instead of at two levels as in Fasel's approach. The consideration of computer storage may be a critical one when three-dimensional calculations are attempted. Both schemes involve systems of nonlinear algebraic equations which must be solved iteratively.

The work presented here describes the details of the problem formulation and numerical solution procedure as applied to spatially periodic, parallel flows. Comparisons with the results of linear analysis are made and verify the correctness of the numerical solutions. Finally, the effects of large amplitude on subcritical stability are investigated and indicate that non-linear effects can be destabilizing.

2. THE MATHEMATICAL FORMULATION

The motion of the fluid is assumed to be described by the two-dimensional, incompressible, time-dependent Navier-Stokes equations. Normalizing the spatial distances by the momentum thickness of the boundary layer, δ, the velocities by the free stream value, U_∞, and time by δ/U_∞, the equations of motion become

$$\frac{\partial u}{\partial t} + u\frac{\partial u}{\partial x} + v\frac{\partial u}{\partial y} + \frac{\partial p}{\partial x} = \frac{1}{R}\nabla^2 u \tag{1}$$

$$\frac{\partial v}{\partial t} + u\frac{\partial v}{\partial x} + v\frac{\partial v}{\partial y} + \frac{\partial p}{\partial y} = \frac{1}{R}\nabla^2 v \tag{2}$$

$$\frac{\partial u}{\partial x} + \frac{\partial v}{\partial y} = 0 \quad . \tag{3}$$

Here, x and u are the coordinate and velocity in the streamwise direction, y and v are the coordinate and velocity in the direction normal to the boundary, p is the fluid pressure divided by the mass density, and $R = U_\infty\delta/\nu$ is the Reynolds number, where ν is the kinematic viscosity. The Laplacian operator is

$$\nabla^2 = \frac{\partial^2}{\partial x^2} + \frac{\partial^2}{\partial y^2} \quad .$$

It is convenient to define a base flow, denoted by capital letters, that satisfies the steady flow equations

$$U\frac{\partial U}{\partial x} + V\frac{\partial U}{\partial y} + \frac{\partial P}{\partial x} = \frac{1}{R}\nabla^2 U \tag{4}$$

$$U\frac{\partial V}{\partial x} + V\frac{\partial V}{\partial y} + \frac{\partial P}{\partial y} = \frac{1}{R}\nabla^2 V \tag{5}$$

$$\frac{\partial U}{\partial x} + \frac{\partial V}{\partial y} = 0 \ . \tag{6}$$

For high Reynolds number flows, these equations can be solved either directly or by using boundary-layer/potential flow techniques. Disturbances to the base flow then satisfy

$$\frac{\partial u'}{\partial t} + U\frac{\partial u'}{\partial x} + u'\frac{\partial U}{\partial x} + u'\frac{\partial u'}{\partial x} + V\frac{\partial u'}{\partial y} + v'\frac{\partial U}{\partial y} + v'\frac{\partial u'}{\partial y}$$

$$+ \frac{\partial p'}{\partial x} = \frac{1}{R}\nabla^2 u' \tag{7}$$

$$\frac{\partial v'}{\partial t} + U\frac{\partial v'}{\partial x} + u'\frac{\partial V}{\partial x} + u'\frac{\partial v'}{\partial x} + V\frac{\partial v'}{\partial y} + v'\frac{\partial V}{\partial y} + v'\frac{\partial v'}{\partial y}$$

$$+ \frac{\partial p'}{\partial y} = \frac{1}{R}\nabla^2 v' \tag{8}$$

$$\frac{\partial u'}{\partial x} + \frac{\partial v'}{\partial y} = 0 \ . \tag{9}$$

The boundary conditions appropriate to these equations are that the disturbance quantities vanish far from the solid boundary,

$$u', v', p' \to 0 \quad \text{as} \quad y \to \infty \ , \tag{10}$$

the disturbance velocities vanish on the solid boundary,

$$u' = v' = 0 \quad \text{at} \quad y = 0 \ , \tag{11}$$

and, by evaluating (8) on the boundary and using (9), that

$$\frac{\partial p'}{\partial y} = -\frac{1}{R}\frac{\partial^2 u'}{\partial x \partial y} \quad \text{at} \quad y = 0 \ . \tag{12}$$

Boundary conditions in the streamwise direction depend on the nature of the problem being solved.

The techniques developed in this work are capable of solving the disturbance equations for the most general base flows, but here we shall consider the special case of parallel flow, when $U = U(y)$ and $V = 0$. Strictly speaking, the only such flow satisfying this condition is the parabolic distribution. In the thin boundary layers that form at high Reynolds numbers, however, the normal velocity field is extremely small and the assumption of parallel flow is nearly met (Schlichting, 1960, p116ff). The disturbance equations can then be simplified to the form

$$\frac{\partial u'}{\partial t} + U\frac{\partial u'}{\partial x} + u'\frac{\partial u'}{\partial x} + v'\frac{dU}{dy} + v'\frac{\partial u'}{\partial y} + \frac{\partial p'}{\partial x} = \frac{1}{R}\nabla^2 u' \tag{13}$$

$$\frac{\partial v'}{\partial t} + U\frac{\partial v'}{\partial x} + u'\frac{\partial v'}{\partial x} \qquad + v'\frac{\partial v'}{\partial y} + \frac{\partial p'}{\partial y} = \frac{1}{R}\nabla^2 v' \tag{14}$$

$$\frac{\partial u'}{\partial x} + \frac{\partial v'}{\partial y} = 0 \ . \tag{15}$$

The linearized form of equations (13) - (15) have been extensively studied, especially the growth rates and spectral properties of periodic disturbances. The assumptions of linearization and periodicity allows the equations above to be transformed into a single ordinary differential equation, the Orr-Sommerfeld equation. The resulting body of knowledge, known as linear stability theory (LST), offers a quantitative test of the direct numerical solution of the equations.

The results discussed in this work are for parallel flows in which U is taken as the horizontal component of the velocity

over a flat plate, the Blasius profile. In order to compare with LST, the disturbance flow is assumed to be periodic with wavelength λ in the streamwise direction. There are then two parameters describing small amplitude motion, the Reynolds number, R, and the dimensionless wavenumber $\alpha = 2\pi\delta/\lambda$.

3. THE NUMERICAL SOLUTION TECHNIQUE

The equations (13), (14), and (15) subject to boundary conditions (10), (11), and (12) are to be solved in a region $0 \leq x \leq \lambda/\delta$ and $0 \leq y < \infty$. The region is first divided into finite sized cells, of constant size in the horizontal and variably spaced in the vertical (see Figure 1). Within each cell, the horizontal velocity is defined at the center of the left face, the vertical velocity at the center of the bottom face, and the pressure at the cell center (see Figure 2).

The following finite-difference form was used to represent the time rate of change of the discrete velocities

$$
\begin{aligned}
\left(\frac{\partial u}{\partial t}\right)_{i,j} = & - \frac{1}{2\delta x} U_j \left(u_{i+1,j} - u_{i-1,j}\right) \\
& - \frac{1}{4\delta x} \Big[u_{i+1,j} \left(u_{i+1,j} + u_{i+1,j}\right) \\
& - u_{i-1,j} \left(u_{i,j} + u_{i-1,j}\right)\Big] \\
& - \frac{1}{4\delta y_j} \Big[u_{i,j+1} \left(v_{i,j+1} + v_{i-1,j+1}\right) \\
& - u_{i,j-1} \left(v_{i,j} + v_{i-1,j}\right)\Big] \\
& - \frac{1}{4}\left(\frac{dU}{dy}\right)_j \left(v_{i,j} + v_{i,j+1} + v_{i-1,j} + v_{i-1,j+1}\right) \\
& - \frac{1}{\delta x} \left(p_{i,j} - p_{i-1,j}\right)
\end{aligned}
$$

(continued)

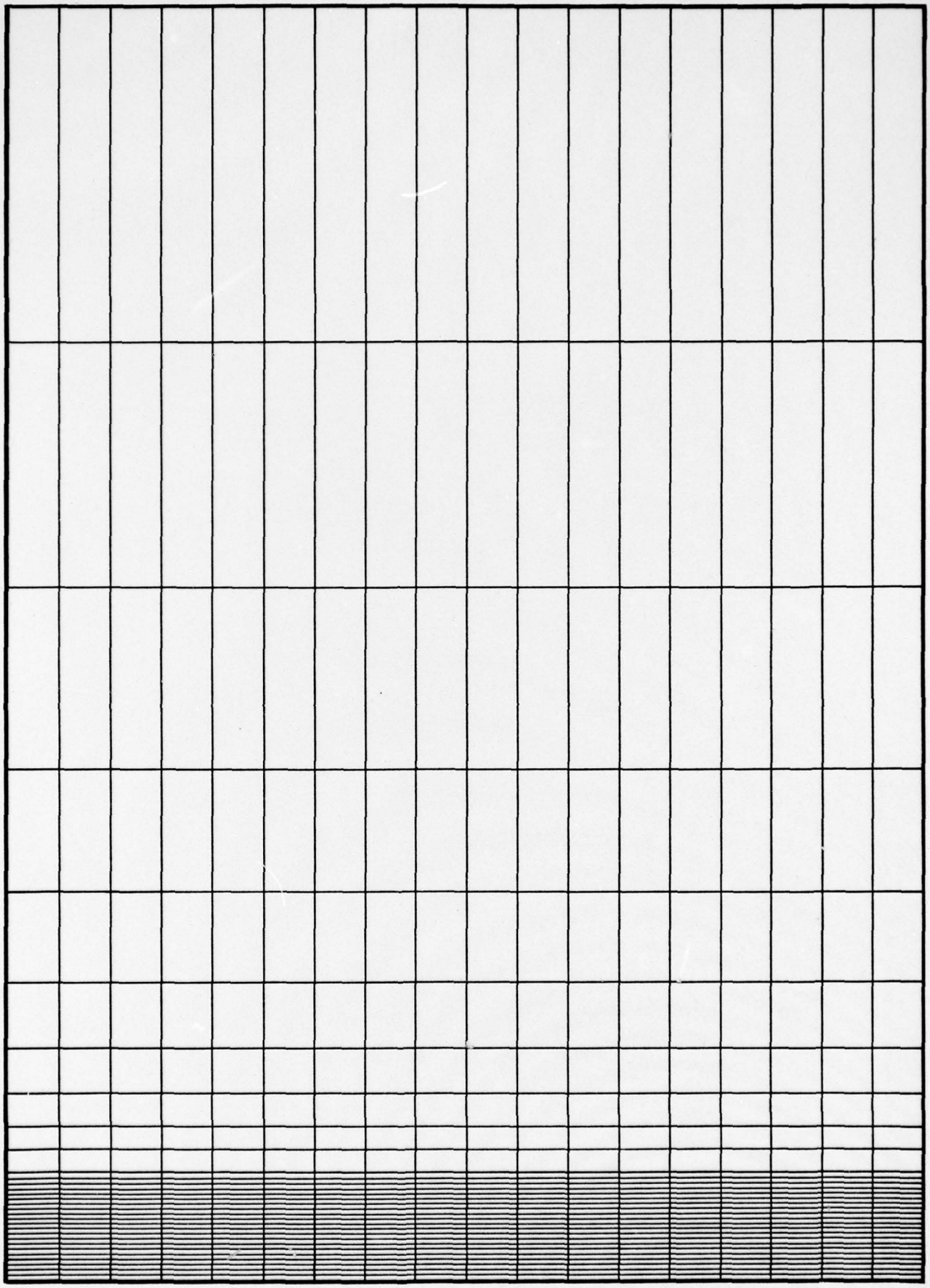

Figure 1. A Typical Finite-Difference Mesh Configuration

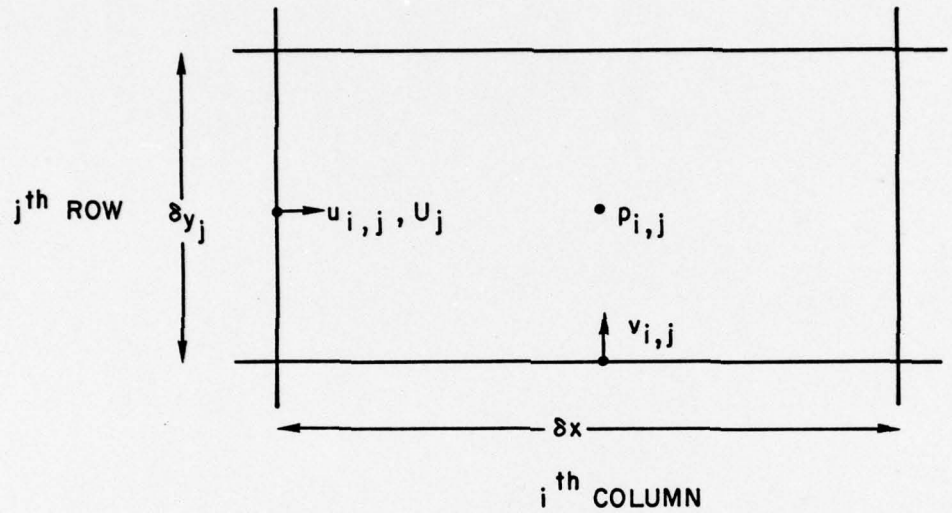

Figure 2. Variable Placement Within a Finite-Difference Cell

$$+ \frac{1}{R(\delta x)^2} (u_{i+1,j} - 2u_{i,j} + u_{i-1,j})$$

$$+ \frac{1}{R\delta y_j} \left[\frac{1}{\delta y_{j+\frac{1}{2}}} (u_{i,j+1} - u_{i,j})\right.$$

$$\left. - \frac{1}{\delta y_{j-\frac{1}{2}}} (u_{i,j} - u_{i,j-1})\right] \tag{16}$$

$$\left(\frac{\partial v}{\partial t}\right)_{i,j} = - \frac{1}{4\delta x} (U_j + U_{j-1})(v_{i+1,j} - v_{i-1,j})$$

$$- \frac{1}{4\delta x} \left[v_{i+1,j} (u_{i+1,j} + u_{i+1,j-1})\right.$$

$$\left. - v_{i-1,j} (u_{i,j} + u_{i,j-1})\right]$$

$$- \frac{1}{4\delta y_{j-\frac{1}{2}}} \left[v_{i,j+1} (v_{i,j} + v_{i,j+1})\right.$$

$$\left. - v_{i,j-1} (v_{i,j} + v_{i,j-1})\right] - \frac{1}{\delta y_{j-\frac{1}{2}}} (p_{i,j} - p_{i,j-1})$$

$$+ \frac{1}{R(\delta x)^2} (v_{i+1,j} - 2v_{i,j} + v_{i-1,j})$$

$$+ \frac{1}{R\delta y_{j-\frac{1}{2}}} \left[\frac{1}{\delta y_j} (v_{i,j+1} - v_{i,j})\right.$$

$$\left. - \frac{1}{\delta y_{j-1}} (v_{i,j} - v_{i,j-1})\right]. \tag{17}$$

Here $\delta y_{j-\frac{1}{2}} = \frac{1}{2}(\delta y_j + \delta y_{j-1})$. Also, we have dropped the prime from the lower case quantities since no confusion with total velocities or pressures can result. The difference form used for the nonlinear terms is that of Piacsek and Williams (1970).

If I and J represent the total number of columns and rows used, with columns i=1 and I and rows j=1 and J being boundary cells outside the physical domain, then the boundary conditions become

$$v_{i,J} = 0 \ , \quad u_{i,J} = -u_{i,J-1} \ , \quad p_{i,J} = -p_{i,J-1} \tag{18}$$

$$v_{i,2} = 0 \ , \quad u_{i,1} = -u_{i,2} \ ,$$

$$p_{i,1} = p_{i,2} + \frac{2}{R\delta x}(u_{i+1,2} - u_{i,2}) \tag{19}$$

$$u_{I,j} = u_{2,j} \ , \quad v_{I,j} = v_{2,j} \ , \quad p_{I,j} = p_{2,j} \tag{20}$$

$$u_{1,j} = u_{I-1,j} \ , \quad v_{1,j} = v_{I-1,j} \ , \quad p_{1,j} = p_{I-1,j} \ . \tag{21}$$

The pressure field is determined so as to guarantee that equation (15) is satisfied. Before discussing the details of how the pressure is calculated, it is convenient to define the tilda finite-difference operators

$$\left(\frac{\partial u}{\partial t}\right)_{i,j} = \left(\frac{\partial \tilde{u}}{\partial t}\right)_{i,j} - \frac{1}{\delta x}(p_{i,j} - p_{i-1,j}) \tag{22}$$

$$\left(\frac{\partial v}{\partial t}\right)_{i,j} = \left(\frac{\partial \tilde{v}}{\partial t}\right)_{i,j} - \frac{1}{\delta y_{j-\frac{1}{2}}}(p_{i,j} - p_{i,j-1}) \ , \tag{23}$$

that is, they are the time rate of change operators without the pressure terms. The solutions are advanced in time by the time-average, implicit algorithm

$$\phi_{i,j}^{n+1} = \phi_{i,j}^{n} + \frac{1}{2}\delta t \left[\left(\frac{\partial \phi}{\partial t}\right)_{i,j}^{n} + \left(\frac{\partial \phi}{\partial t}\right)_{i,j}^{n+1} \right] , \tag{24}$$

where the superscript indicates the time level and δt is the finite time step. This scheme when used with central, space differencing introduces no numerical dissipation (Roach, 1976, p.84). The velocity fields are then given by the formulae

$$u_{i,j}^{n+1} = u_{i,j}^{n} + \frac{1}{2}\delta t \left[\left(\frac{\partial u}{\partial t}\right)_{i,j}^{n} + \left(\frac{\partial \tilde{u}}{\partial t}\right)_{i,j} \right] - \frac{\delta t}{2\delta x} \left(p_{i,j}^{n+1} - p_{i-1,j}^{n+1}\right) \tag{25}$$

$$\equiv \tilde{u}_{i,j} - \frac{\delta t}{2\delta x} \left(p_{i,j}^{n+1} - p_{i-1,j}^{n+1}\right) \tag{26}$$

and

$$v_{i,j}^{n+1} = v_{i,j}^{n} + \frac{1}{2}\delta t \left[\left(\frac{\partial v}{\partial t}\right)_{i,j}^{n} + \left(\frac{\partial \tilde{v}}{\partial t}\right)_{i,j} \right] - \frac{\delta t}{2\delta y_{j-\frac{1}{2}}} \left(p_{i,j}^{n+1} - p_{i,j-1}^{n+1}\right) \tag{27}$$

$$\equiv \tilde{v}_{i,j} - \frac{\delta t}{2\delta y_{j-\frac{1}{2}}} \left(p_{i,j}^{n+1} - p_{i,j-1}^{n+1}\right) . \tag{28}$$

Because the time derivatives involve products of the fluid velocities, (26) and (28) are coupled, nonlinear algebraic equations. Furthermore, the pressure field at the new time level must be chosen so that the new velocities are divergence free, that is

$$\frac{1}{\delta x} \left(u_{i+1,j}^{n+1} - u_{i,j}^{n+1}\right) + \frac{1}{\delta y_j} \left(v_{i,j+1}^{n+1} - v_{i,j}^{n+1}\right) = 0 . \tag{29}$$

This last relation leads to the following linear, elliptic boundary value problem for the pressures

$$\frac{1}{(\delta x)^2}\left[p^{n+1}_{i+1,j} - 2p^{n+1}_{i,j} + p^{n+1}_{i-1,j}\right]$$

$$+ \frac{1}{\delta y_j}\left[\frac{1}{\delta y_{j+\frac{1}{2}}}\left(p^{n+1}_{i,j+1} - p^{n+1}_{i,j}\right)\right.$$

$$\left. - \frac{1}{\delta y_{j-\frac{1}{2}}}\left(p^{n+1}_{i,j} - p^{n+1}_{i,j-1}\right)\right]$$

$$= \frac{2}{\delta t}\left[\frac{1}{\delta x}\left(\tilde{u}_{i+1,j} - \tilde{u}_{i,j}\right) + \frac{1}{\delta y_j}\left(\tilde{v}_{i,j+1} - \tilde{v}_{i,j}\right)\right] \quad (30)$$

The solution is advanced to the n+1 st time step through the following iterative scheme

1. The new velocities and pressures are set equal to the previous values.
2. The tilda velocities are computed using (25) - (28).
3. The system of equations (30) is inverted to obtain a better guess of the pressure.
4. Equations (26) and (28) are used to obtain a better guess of the velocities
5. Steps (2), (3), and (4) are repeated until the quantities do not change by some predetermined amount.

The solution of (30) is obtained by decomposing and backsolving the banded pressure matrix using the Cholesky method. The manipulations are carried out by an especially efficient routine developed by M. Vander Vorst of JAYCOR.

Stability of the solution requires that the time step does not exceed values imposed by the advection and diffusion terms.

$$\delta t < \min\left\{\frac{\delta x}{|U_j + u_{i,j}|}, \frac{\delta y_j}{|v_{i,j}|}, \frac{R}{4}(\delta x)^2, \frac{R}{4}(\delta y_j)^2\right\} \tag{31}$$

Experience has shown that if δt is taken to be one-quarter of the maximum time step allowed, then at least three significant figures are obtained in the velocity and pressure fields with five iterations.

4. COMPARISON WITH LINEAR STABILITY THEORY

The linearized form of equations (13) - (15) have been studied in detail, e.g., Wazzan, et al., (1968), Jordinson (1970), the case of greatest interest being when U takes on the Blasius profile. See also the reviews by Tani (1969) and Reshotko (1976). Not only have detailed quantitative solutions been obtained, but the predicted fluid dynamic behavior is in close agreement with experimental observation of small disturbances in the boundary layer of a flat plate. For example, see Ross, et al., (1970). Comparison with LST offers then a meaningful test of the numerical approach.

When the disturbances are periodic in space, the eigenfunctions are characterized by the two parameters α and R. Figure 3 shows the curve of neutral stability, that is those distrubances which neither grow nor die out, as determined by Jordinson; points inside the curve are unstable flows, those outside are stable. Below the critical Reynolds number of 520, LST predicts that all disturbances die out and thus that the boundary layer is completely stable.

To compare with the predictions of LST a series of numerical experiments were conducted. In each case the mesh consisted of 18 constant-sized cells in the horizontal, periodic direction and 34 variably-sized cells in the vertical. The smallest vertical cells were 0.1δ wide, while above $y = 2.0\delta$ the cells expanded geometrically so that the top of the last cell was almost 100δ from the solid boundary. Figure 1 shows the mesh configuration up to $y = 25\delta$. The top boundary appears to not influence the results, since placing it further away led to no change in the flow properties. The base flow was given a small disturbance which was then allowed to evolve toward a final state.

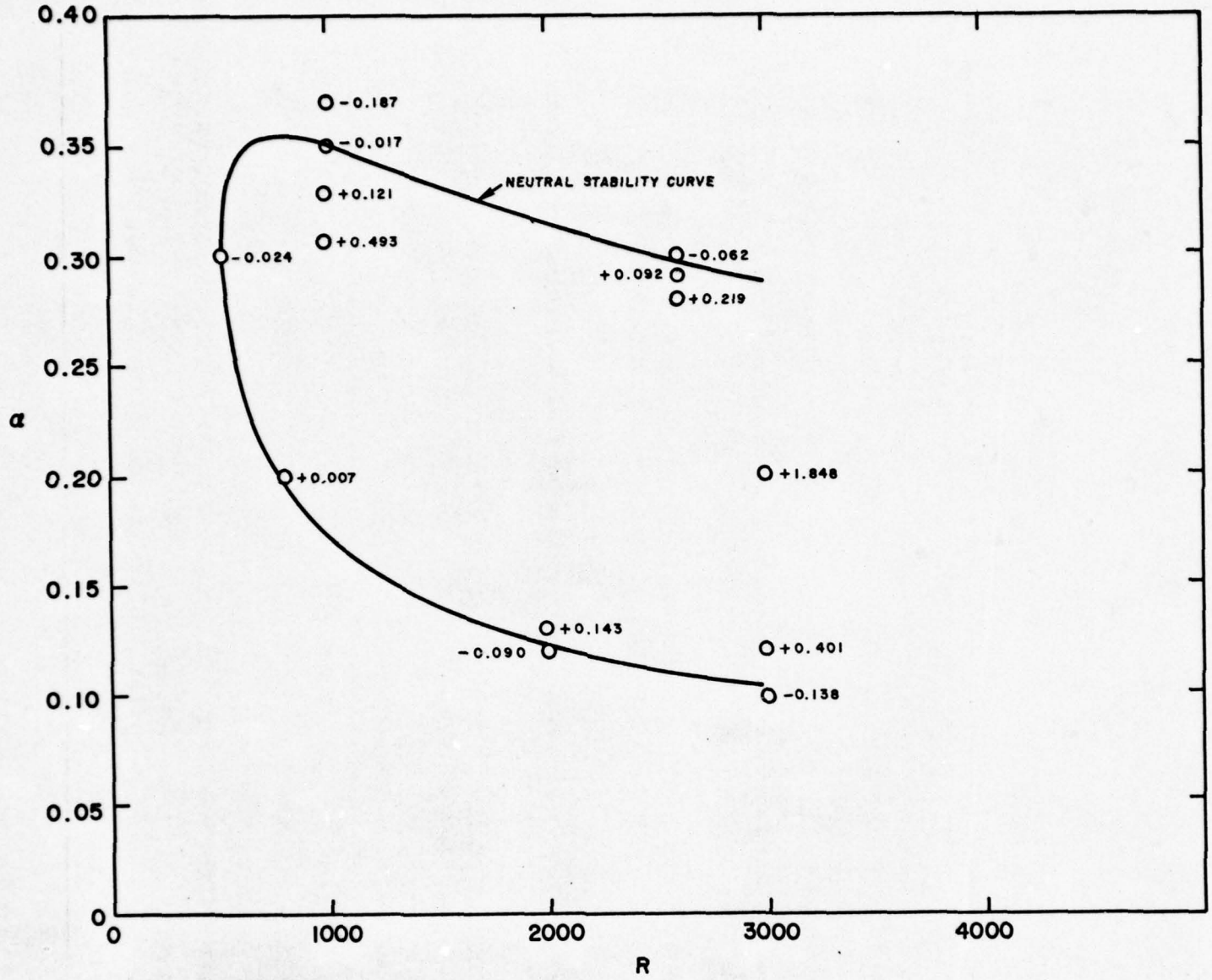

Figure 3. Neutral Stability Curve and Cases for which Numerical Calculations have been made. Numbers indicate the logarithmic energy change per period.

The circles shown in Figure 3 represent the matrix of numerical experiments conducted. The numbers indicate the logarithmic energy change per period of oscillation

$$\theta = \ln \frac{E(t+T)}{E(t)} \ , \ T = \text{period of disturbance.} \tag{32}$$

This quantity has not yet reached a final value in all cases, so the quoted value, taken at the end of a run, may change slightly. Figure 4 shows the variation with time of the energy for most of the runs.

Figure 5 compares the time variation of production and dissipation for one case near the neutral curve, where

$$\text{production} = \iint dx\, dy \left(- uv \frac{dU}{dy} \right) \tag{33}$$

$$\text{dissipation} = -\iint dx\, dy \left(u\nabla^2 u + v\nabla^2 v \right) . \tag{34}$$

The production is the rate at which energy is extracted from the base flow, while dissipation is the rate at which it is lost to heat. The rates should be equal for a neutral case. Since the initial disturbance is not a pure eigenmode of the system, and since neighboring modes die out slowly, the flow requires a considerable time to settle into a single, pure motion. That difference distinguishes a true initial value problem from the eigenvalue problem posed by LST.

Since negative values in Figure 3 indicate damped motion and positive values indicate growth, the results are not in conflict with LST. In fact, when nearby pairs of numerical calculations, one showing growth and the other decay, are used to interpolate a neutral condition, the results agree with LST to within a few percent for both the wavenumber and frequency, see Table 1. Here, β is the dimensionless frequency of oscillation. The numerical calculation appears to have correctly reproduced the overall energy balance and time behavior in the flow.

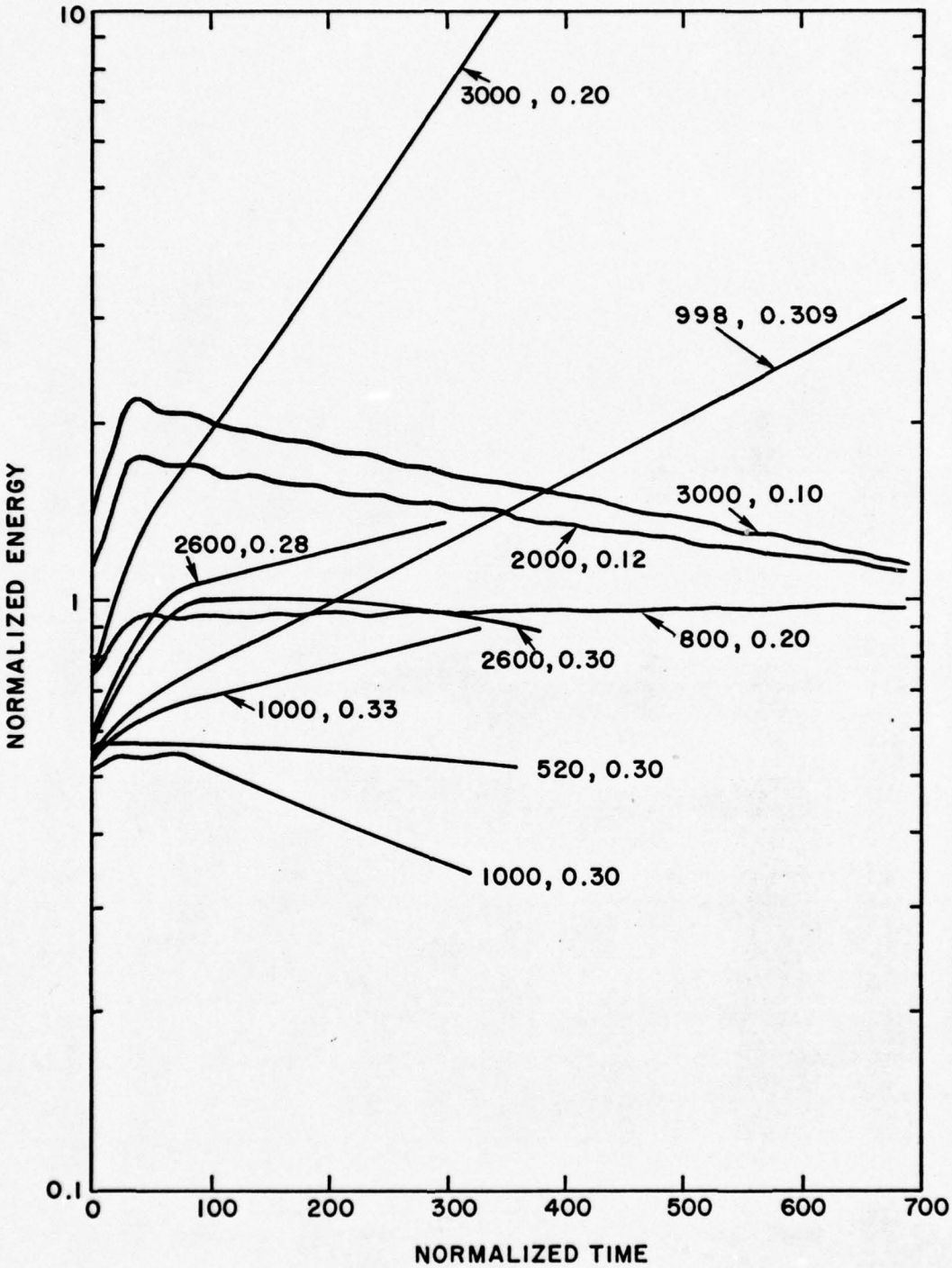

Figure 4. Time variation of the flow energy for several numerical calculations.

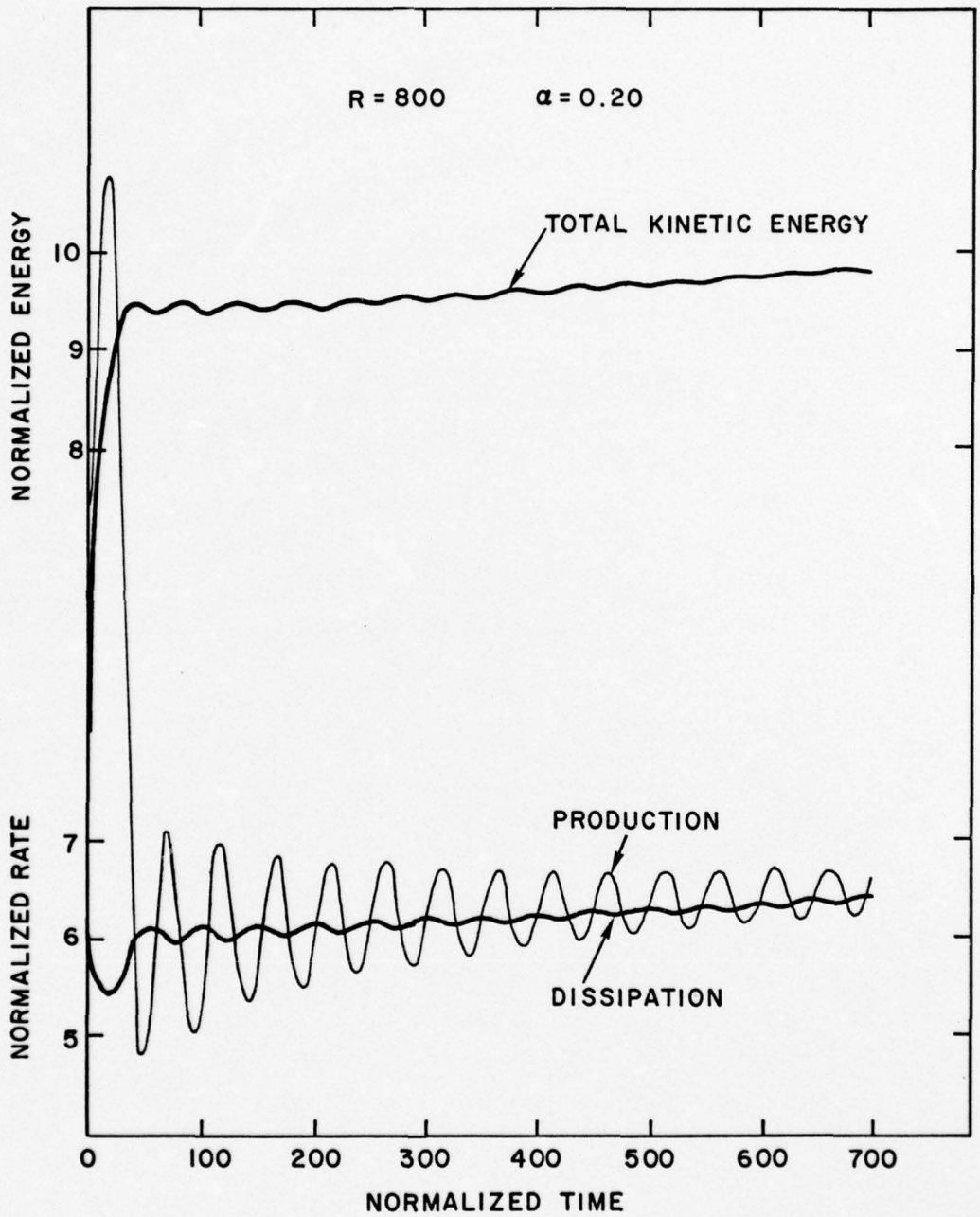

Figure 5. Comparison of Production and Dissipation Rates During the Relaxation to a Final State for a Case Near the Neutral Curve.

Table 1.

R		α	β
1000	numerical	0.348	0.128
	LST	0.351	0.131
2000	numerical	0.1239	0.0327
	LST	0.1234	0.0332
2600	numerical	0.295	0.0927
	LST	0.297	0.0947
3000	numerical	0.1051	0.0257
	LST	0.1029	0.0235

α		R	β
0.30	numerical	530	0.1167
	LST	521	0.1175

Next, details of the flow field were examined. Figure 6 shows the variation with time of the horizontal disturbance velocity at a particular streamwise position and for various distances from the wall. This format is analogous to the continuous output of a velocity probe and shows the experimentally observed pattern (Schlichting, 1969, p.403) that the amplitude grows with distance from the wall, reaches a peak, suffers a phase reversal, and dies out. The calculated period of oscillation is 93.79 while the theoretical value is 93.48.

Figures (7) and (8) compare the amplitude and phase variation with distance from the wall found from a numerical calculation and Jordinson's eigenfunction solution. The comparison shows that the details of the flow are reproduced completely, including the subtle phase variations occurring in the flow near the wall. The numerical calculation appears to have correctly reproduced the flow details as well as the overall energy balances.

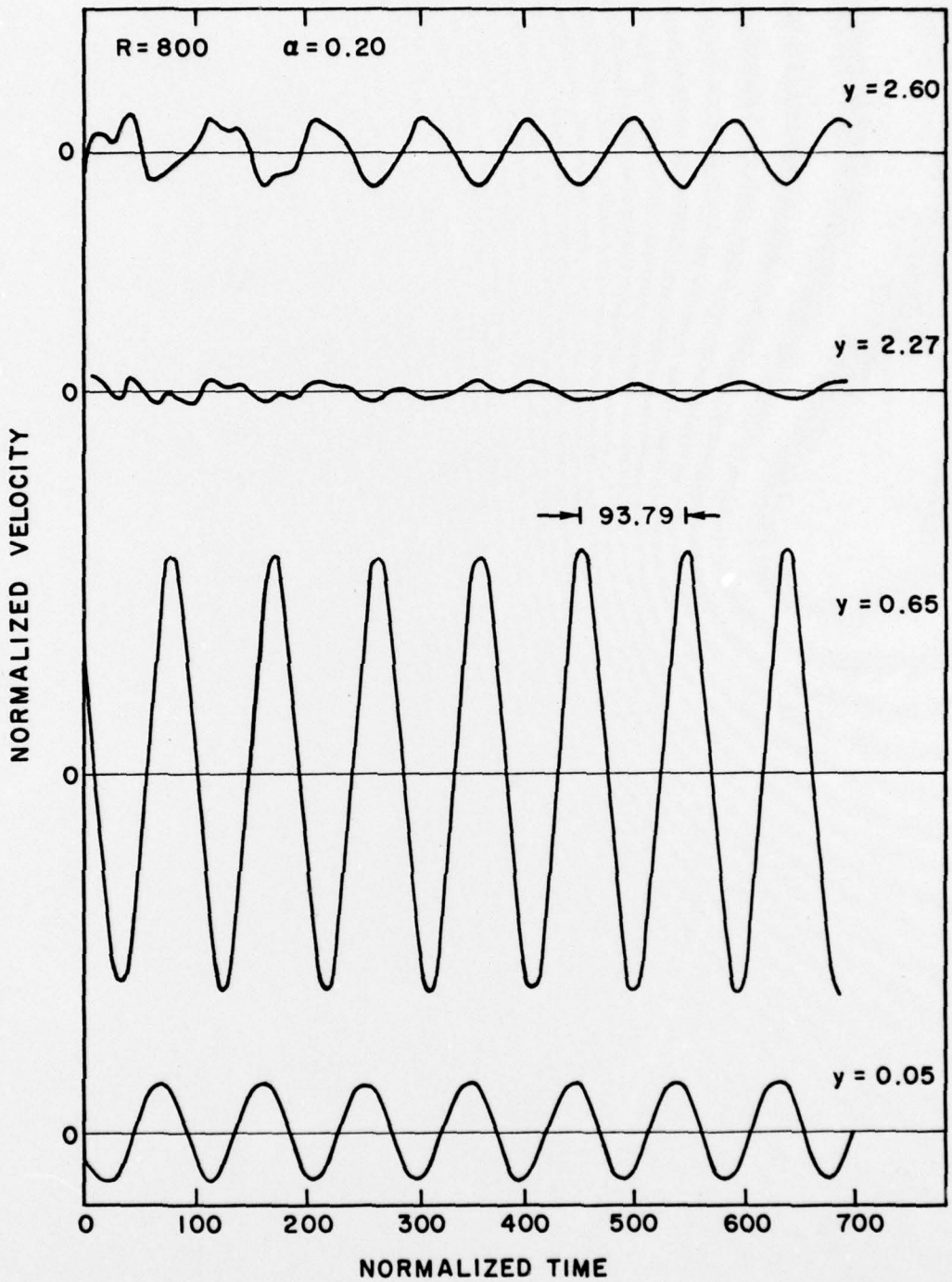

Figure 6. Time Traces of the Horizontal Velocity Component for Various Distances from the Wall.

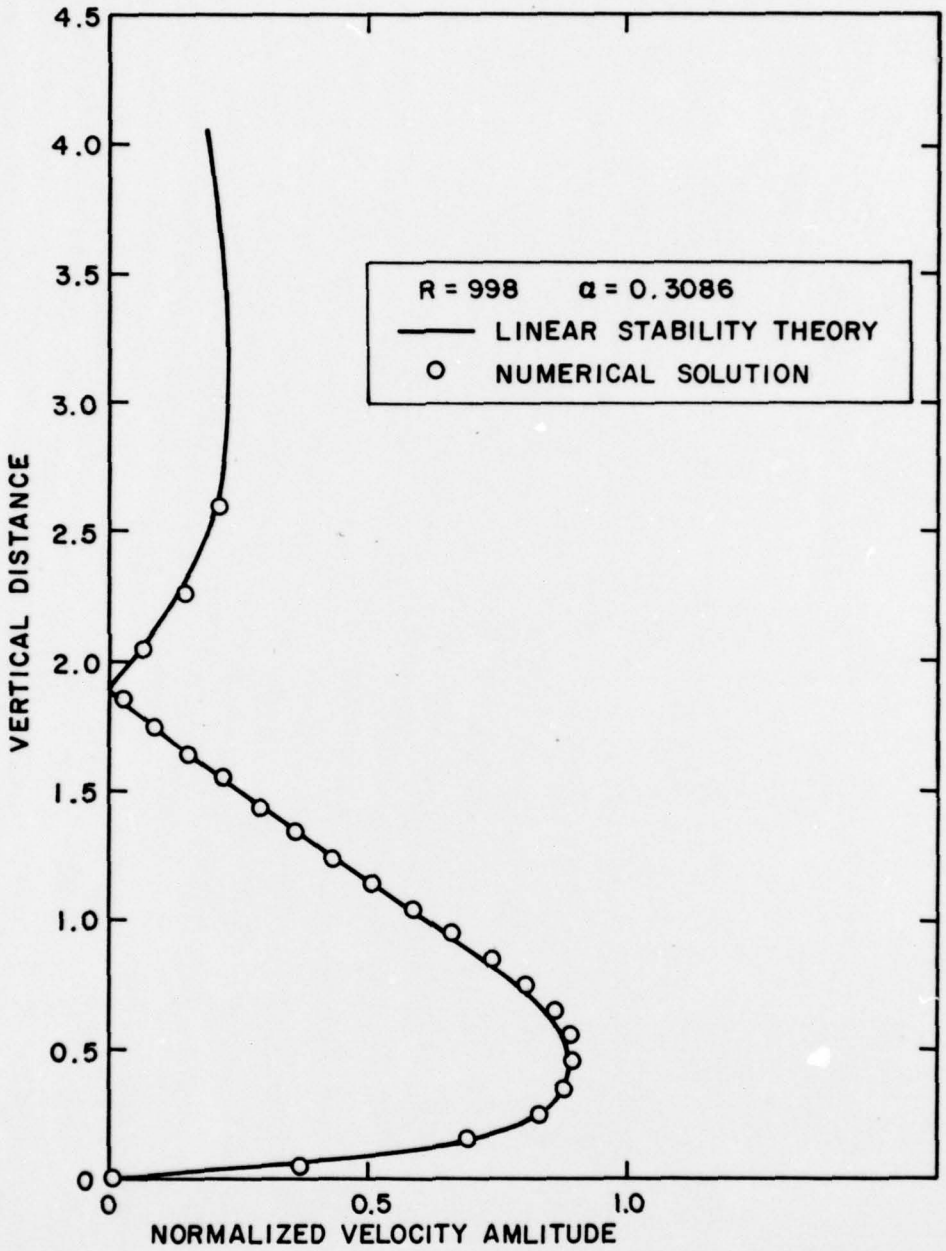

Figure 7. Comparison of Horizontal Velocity Amplitude Variation.

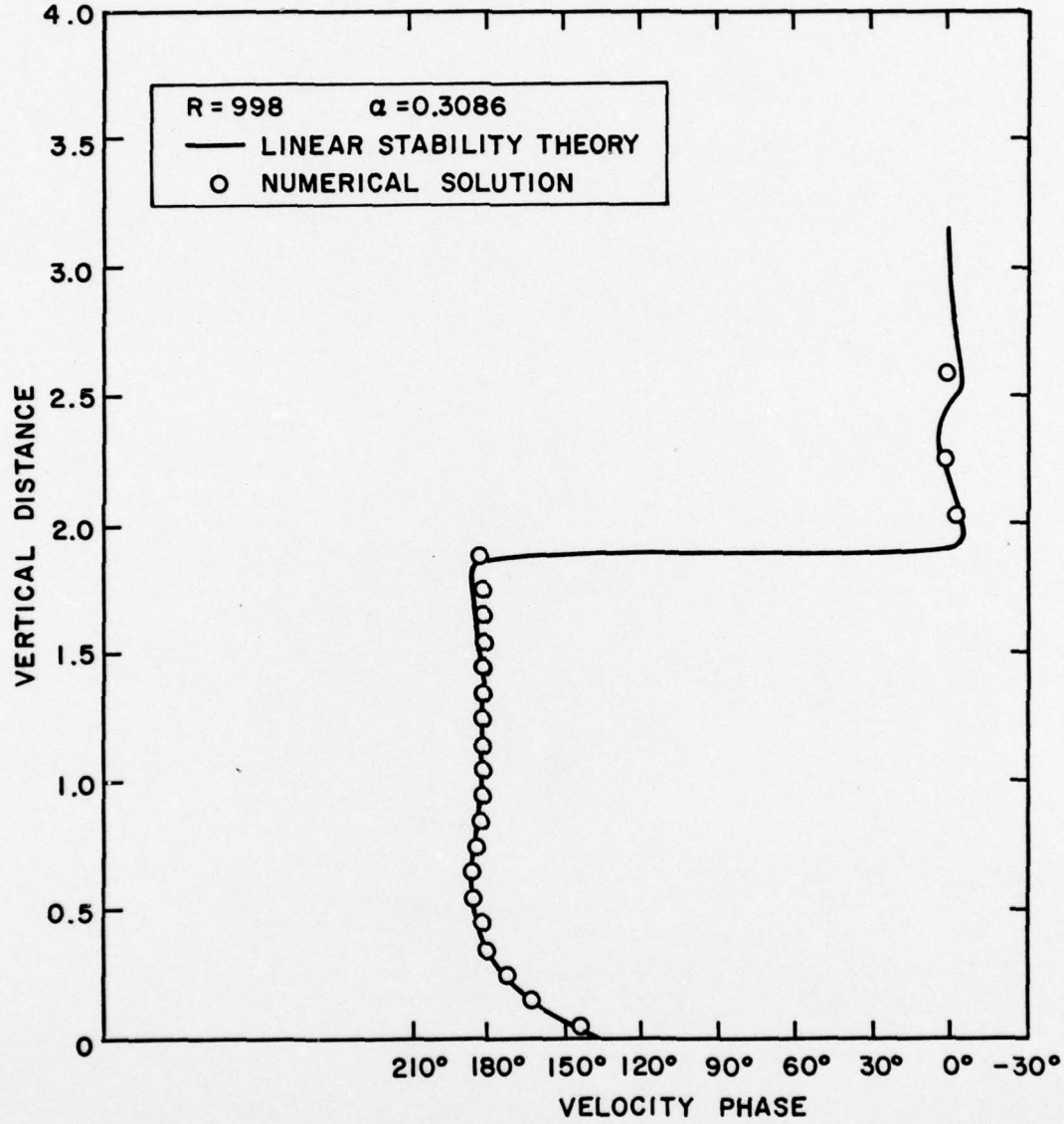

Figure 8. Comparison of Horizontal Velocity Phase Variation.

5. FINITE AMPLITUDE EFFECTS

The previous comparisons with linear stability theory suggest that the behavior of small amplitude disturbances is being correctly computed numerically. A series of calculations was then performed to determine the effects of finite amplitude. In each case the initial disturbance had the same spatial distribution but the maximum amplitude of u' was taken as 0.0001, 0.01, 0.03, and 0.1 of U_∞. The results show a trend conjectured by nonlinear stability theories (Stewartson, 1975) that finite amplitude effects can be destabilizing.

Figure 9 shows the variation of the total energy in the disturbance flow in each case, normalized to the same initial value. The case considered is $R = 500$, $\alpha = 0.30$, a point in the subcritical regime where LST predicts all disturbances to die out. At the smallest amplitudes the disturbance dies out at a rate consistant with LST. For $u' = 0.03$, however, the decay has been noticeably decreased, while for $u' = 0.1$ the disturbance is almost neutrally stable. Although a truly unstable state was not achieved, the destabilizing effects seem to be definite. A similar variation is seen for unstable small amplitude modes: as they grow to finite amplitude the rate of growth increases.

Figure 10 further illustrates the effects of finite amplitude, by considering the integrated production and dissipation rates for the case $R = 500$, $\alpha = 0.30$. At small amplitudes dissipation always exceeds production and the disturbance monotonically dies out. At $u' = 0.1$, however, the production exceeds dissipation during part of the oscillation, so that for some time it grows and for some time it is damped. The damped periods are greater so that the disturbance is dying out overall, but a balance is almost being struck.

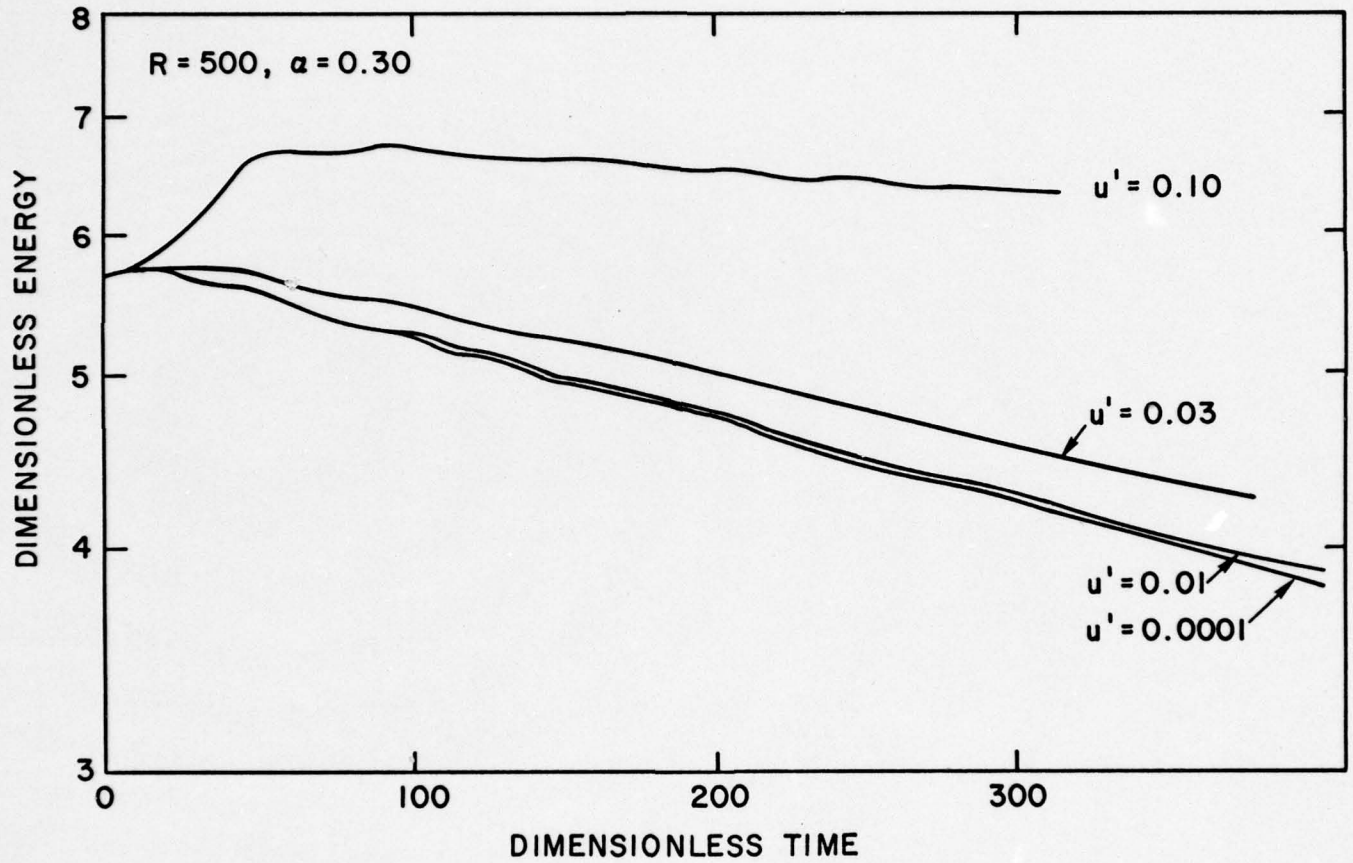

Figure 9. Variation of Energy with Time for Various Amplitudes of the Initial Disturbance.

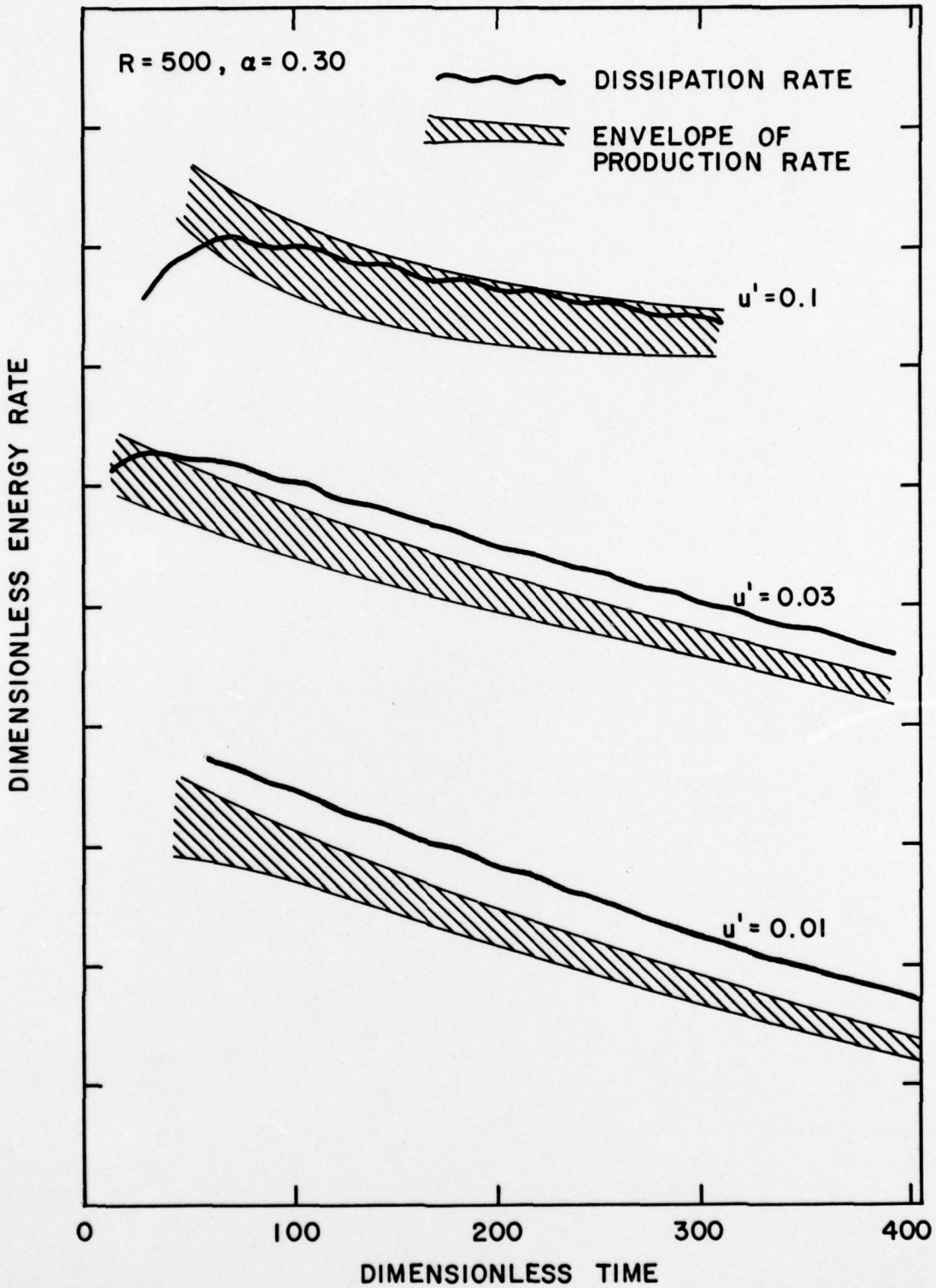

Figure 10. Variation of Production and Dissipation Rates for Various Initial Disturbance Amplitudes.

The accuracy of finite difference techniques for large amplitude phenomena is difficult to assess and so a detailed investigation is probably not warranted at this time. Still, the results, indicate that the numerical solution technique used in this work may be a useful tool in studying finite amplitude effects in the boundary layer.

6. CONCLUDING REMARKS

The finite-difference method presented here has been shown to accurately reproduce analytical results concerning boundary layer stability with a modest storage requirement (612 interior cells) and modest computational time (typically 2 - 5 minutes of CDC 7600 central processor time). This efficiency, coupled with encouraging results in the nonlinear regime, makes the approach an attractive candidate for studying the large amplitude, three-dimensional motion that accompanies boundary-layer transition.

7. ACKNOWLEDGEMENTS

This research was sponsored by the Space and Missile Systems Organization and the Air Force Office of Scientific Research (AFSC), United States Air Force, under Contract No. F49620-77-C-0030. The United States Government is authorized to reproduce and distribute reprints for governmental purposes notwithstanding any copyright notation hereon.

8. REFERENCES

1. Fasel, H. (1976), "Investigation of the stability of boundary layers by a finite-difference model of the Navier-Stokes equations," J. Fluid Mech., vol. 78, p.355.

2. Jordinson, R. (1970), "The flat plate boundary layer. Part 1. Numerical integration of the Orr-Sommerfeld equation," J. Fluid Mech., vol. 43, p.801.

3. Murdock, J. W. (1977), "A numerical study of nonlinear effects on boundary-layer stability," AIAA Journal, vol. 15.

4. Piacsek, S. A. and Williams, G. P. (1970), "Conservation properties of convection differencing schemes," J. Comp. Phys., vol. 6, p.392

5. Reshotko, E. (1976), "Boundary-layer stability and transition," in Annual Reviews of Fluid Mechanics, vol. 8, p.311.

6. Roache, P. J. (1976), Computational Fluid Dynamics, Hermosa Publishers, Albuquerque.

7. Ross, J. A., Barnes, F. H., Burns, J. G., and Ross, M. A. S. (1970), "The flat plate boundary layer. Part 3. Comparison of theory with experiment," J. Fluid Mech., vol. 43, p.819.

8. Schlichting, H. (1960), Boundary Layer Theory, 4th ed., McGraw-Hill.

9. Stewartson, K. (1975), "Some aspects of nonlinear stability theory," Polish Academy of Sciences, vol. 7, p.101.

10. Tani, I. T. (1969), "Boundary-layer transition," in Annual Reviews of Fluid Mechanics, vol. 1, p.169.

11. Wazzan, A. R., Okamura, T. T., and Smith, A. M. O. (1968), "Spatial and temporal stability charts for the Falkner-Skan boundary-layer profiles," McDonald-Douglas Co. Report No. DAC-67086.

UNCLASSIFIED

SECURITY CLASSIFICATION OF THIS PAGE (When Data Entered)

REPORT DOCUMENTATION PAGE	READ INSTRUCTIONS BEFORE COMPLETING FORM
1. REPORT NUMBER: AFOSR-TR- 78-0062	2. GOVT ACCESSION NO. / 3. RECIPIENT'S CATALOG NUMBER
4. TITLE (and Subtitle): NUMERICAL CALCULATION OF THE STABILITY OF PARALLEL FLOWS.	5. TYPE OF REPORT & PERIOD COVERED: FINAL rept. 1 Jan 77 - 31 Oct 77
	6. PERFORMING ORG. REPORT NUMBER
7. AUTHOR(s): JAMES H. STUHMILLER	8. CONTRACT OR GRANT NUMBER(s): F49620-77-C-0030
9. PERFORMING ORGANIZATION NAME AND ADDRESS: JAYCOR, 1401 CAMINO DEL MAR (PO BOX 370), DEL MAR, CA 92014	10. PROGRAM ELEMENT, PROJECT, TASK AREA & WORK UNIT NUMBERS: 2307A1, 61102F
11. CONTROLLING OFFICE NAME AND ADDRESS: AIR FORCE OFFICE OF SCIENTIFIC RESEARCH/NA, BLDG 410, BOLLING AIR FORCE BASE, D C 20332	12. REPORT DATE: 5 Dec 77
	13. NUMBER OF PAGES: 37
14. MONITORING AGENCY NAME & ADDRESS (if different from Controlling Office)	15. SECURITY CLASS. (of this report): UNCLASSIFIED
	15a. DECLASSIFICATION/DOWNGRADING SCHEDULE

16. DISTRIBUTION STATEMENT (of this Report)

Approved for public release, distribution unlimited.

17. DISTRIBUTION STATEMENT (of the abstract entered in Block 20, if different from Report)

18. SUPPLEMENTARY NOTES

19. KEY WORDS (Continue on reverse side if necessary and identify by block number)

BOUNDARY LAYER TRANSITION
NAVIER-STOKES, EQUATIONS
PARALLEL FLOW
FINITE DIFFERENCE COMPUTATION
TWO-DIMENSIONAL FLOW
NON-LINEAR EFFECTS

20. ABSTRACT (Continue on reverse side if necessary and identify by block number)

A numerical approach to solving the two-dimensional, incompressible Navier-Stokes equations is presented and is used to study the stability and evolution of disturbance in a boundary layer. Previous numerical approaches have used streamfunction-vorticity formulations that take advantage of the special properties of two-dimensional flow. The present method solves a finite-difference form of the momentum equations and may therefore be extended to three-dimensions more readily. Computations using this technique are compared with the result of linear stability theory for small amplitude disturbances and are found to give satisfactory agreement, while calculations at large amplitude support the conjecture that non-linear effects can be destabilizing.

DD FORM 1 JAN 73 1473 EDITION OF 1 NOV 65 IS OBSOLETE

UNCLASSIFIED

SECURITY CLASSIFICATION OF THIS PAGE (When Data Entered)

342 228